Jurnal Fisika Unand (JFU)
Vol. 15, No. 2, Maret 2026, hal. 211 – 220
ISSN: 2302-8491 (Print); 2686-2433 (Online)
https://doi.org/10.25077/jfu.15.2.211-220.2026

Open Access

Effect of Electrokinetic Remediation on the Distribution and Concentration of Lead (Pb) in Ex-Mining Land of PT Semen Baturaja Tbk

Rahma Nur Komariah[1], Achmad Chalid Afif Alfajrin[2*], Arien Aisyara[1], Muhammad Akmal Halid[1], Lamtongam Simatupang[1], Hamzah Daffa Ghifari[1], Hendra Prasetia[3], Angga Jati Widiatama[4], Sabar[2], Rhahmi Adni Pesma[2], Rezki Naufan Hendrawan[4], Fadli Hastito[2]

[1]Department of Forestry Engineering, Institut Teknologi Sumatera (ITERA), South Lampung, Lampung 35365, Indonesia
[2]Department of Instrumentation and Automation Engineering, Institut Teknologi Sumatera (ITERA), South Lampung, Lampung 35365, Indonesia
[3]Research Center for Mining Technology, BRIN, South Lampung, Lampung 35361, Indonesia
[4]Department of Engineering Geology, Institut Teknologi Sumatera (ITERA), South Lampung, Lampung 35365, Indonesia

ARTICLE INFO

Article History:
Submitted: 15 January 2026
Revised: 20 February 2026
Accepted: 31 March 2026

Keywords:
Electronic remediation
Heavy metal-contaminated soil
Ion migration
Lead (Pb)
Mining land reclamation

ABSTRACT

Mining activities can lead to the accumulation of heavy metals in soil, particularly lead (Pb), posing risks to ecosystems and human health. PT Semen Baturaja Tbk has implemented revegetation as a post-mining reclamation strategy, but success rates remain low, potentially due to high Pb concentrations in the soil. This study investigates the effectiveness of electrokinetic remediation (EKR) in mobilizing Pb ions in ex-mining soil using aluminum plate electrodes under a 20 V direct current over treatment durations of 24 and 48 hours. Soil moisture was maintained at 900 mL, and Pb concentrations were measured by X-ray fluorescence (XRF). Initial Pb concentrations ranged from 158.9 to 165.0 ppm across soil segments. After 48 hours, Pb concentration near the cathode decreased from 165.0 to 155.1 ppm, while Pb accumulation on the cathode surface increased from 30.8 to 46.9 ppm, confirming active electromigration. However, Pb concentration near the anode increased from 163.3 to 167.0 ppm, attributed to electrochemical oxidation of the aluminum anode. These findings confirm that EKR can initiate directional Pb migration; however, optimizing electrode materials and extending treatment duration are essential to enhance removal efficiency and minimize secondary contamination in future applications.

Copyright © 2026 Author(s).

Corresponding Author:
Achmad Chalid Afif Alfajrin
Email: achmad.alfajrin@ia.itera.ac.id

I. INTRODUCTION

Mining activities have long been recognized as a major source of environmental degradation, primarily through the accumulation of heavy metals in soil, which poses serious risks to both ecosystems and human health. In the cement production process, pollutants such as dioxins, heavy metals, and hazardous particulate matter are often released into the environment (Yahaya et al., 2023). These impacts necessitate the implementation of systematic remediation efforts, especially by mining companies, as mandated by national regulations. According to Ministerial Regulation of Energy and Mineral Resources No. 7 of 2020, every Mining Business License or Special Mining Business License is obliged to develop and execute reclamation and post-mining plans, including the provision of reclamation and post-mining guarantees.

One form of reclamation undertaken by PT Semen Baturaja Tbk is revegetation, utilizing both forestry species such as *Paraserianthes falcataria* (sengon), *Swietenia mahagoni* (mahogany), and *Samanea saman* (trembesi), as well as fruit trees like mango, jackfruit, durian, and *Syzygium aqueum* (water apple) (Hartati et al., 2023). However, the success rate of this revegetation effort remained low, with only 20% of planted species surviving in 2019 (Siregar et al., 2020). This low success rate is attributed to the high concentrations of heavy metals — particularly lead (Pb) — in the soil, which adversely affect plant growth and ecological recovery (Liu et al., 2018). While some heavy metals are essential in trace amounts for plant metabolism, excessive levels can be toxic (Buta et al., 2019). Lead, in particular, can cause chlorosis, inhibit photosynthesis, and disrupt mitochondrial respiration in plants (Mungki & Taufikurahman, 2004).

Moreover, the use of fruit trees in revegetation on contaminated lands raises additional health concerns, as these plants may accumulate heavy metals in their edible parts. Sarie (2019) and Asuquo & Bate (2020) found that fruit-bearing trees such as mangoes can accumulate Pb in their roots, stems, leaves, and fruits, potentially posing significant risks to human health. Chronic exposure to Pb has been linked to liver and kidney damage, as well as cognitive impairment and developmental disorders (Zulfiqar et al., 2017). To mitigate these risks, soil management strategies must be implemented to reduce heavy metal contamination before revegetation efforts commence.

One promising method for soil decontamination is electrokinetic remediation (EKR), which utilizes an electric field to mobilize and remove contaminants such as Pb from the soil matrix. Suied et al. (2018) reported a Pb removal efficiency of 72.49% using steel electrodes, while Devi et al. (2023) achieved removal efficiencies of 63%, 44%, and 31% for various contaminants using a combination of aluminum and iron electrodes in textile-contaminated soils. These studies demonstrate the potential of EKR for in situ heavy-metal remediation.

Despite the growing body of literature on EKR, several critical gaps remain. Most existing studies have focused on artificially spiked soils or industrial wastewater-contaminated media under controlled laboratory conditions (Suied et al., 2018; Devi et al., 2023), which may not accurately represent the physicochemical complexity of real ex-mining soils — particularly those with naturally alkaline pH, high water-holding capacity, and heterogeneous mineral composition, such as those found in limestone-based cement mining areas. Furthermore, while reactive electrodes such as steel and iron have been extensively tested, the performance of aluminum plate electrodes — which are more cost-effective and widely available — remains insufficiently characterized for Pb removal in this specific soil type. The site-specific context also presents a unique knowledge gap: to date, no study has evaluated the applicability of EKR as a pre-reclamation soil treatment strategy at PT Semen Baturaja Tbk, where revegetation success rates have been critically low (20%) due to persistent Pb contamination (Siregar et al., 2020). Addressing this gap is essential, as evidence-based remediation data are needed to guide safe land preparation before agroforestry or food crop cultivation is introduced on post-mining land.

Therefore, this study aims to evaluate the effect of electrokinetic remediation on the distribution and migration of Pb^{2+} ions in ex-mining soil from PT Semen Baturaja Tbk. The remediation system used aluminum plate electrodes at 20 V direct current for two treatment durations: 24 and 48 hours. Unlike previous studies that employed inert or mixed-metal electrodes in non-site-specific soils, this study provides the first empirical assessment of EKR performance under the actual soil and operational conditions of a post-mining reclamation site in South Lampung, Indonesia. The findings are expected

to support the implementation of more effective and safer post-mining land reclamation strategies, particularly in areas intended for agroforestry or food crop cultivation.

II. METHOD

3.1 Materials

This study used the primary material: ex-mining soil from PT Semen Baturaja Tbk. The soil used as a sample was taken from disposal 4 in the mining area of PT Semen Baturaja Tbk. The tools used in the study were WANPTEK DC PSU 3010H power supply with a voltage of 20 V and a maximum current limit of 5 A, Hioki DT4261 digital multimeter, aluminum plate electrode with size of 12 cm x 10 cm x 1 mm, aquarium with size of 30 cm x 10 cm x 10 cm, Sieve Shaker ENDECOTS Octagon 200, Biobase BOV-V429F oven, Hammer Mill, and Raymond Mill. In soil samples and electrodes, Pb concentration was determined by X-ray fluorescence (XRF).

3.2 Sample Preparation

The initial treatment of soil samples is drying and sieving. The soil is dried to remove the initial water content. After drying, the soil is crushed using a Hammer Mill and Raymond Mill. Then, the sample is sieved to 200 mesh using an ENDECOTS Octogon 200 Sieve Shaker. This stage is carried out to standardize the sample conditions prior to treatment and to meet the requirements of the XRF analysis.

3.3 Water Holding Capacity (WHC) Measurements

Water-holding capacity (WHC) measurements on soil samples determine the amount of water to be added in the study. WHC measurement uses a dry soil sample of 50 g (W_0) and the addition of 50 mL of water. The soil sample is placed on filter paper, and then 50 mL of water is poured so that the soil mass becomes 100 g, and the sample is allowed to sit until no more water drips from the filter paper. The water droplets from the filter paper are measured using a beaker, and then the soil mass of 100 g is subtracted from the measured water droplets (W_1). The calculation of WHC uses an equation based on SNI 03-1971-1990 as follows:

$$WHC\% = \frac{W_0 - W_1}{W_1} \times 100\% \quad (1)$$

where:

W_1 = Saturated soil mass (g)

W_0 = Dried soil mass (g)

3.4 Resistance Measurement

The determination of soil resistance was conducted using an experimental setup consisting of 1500 g of soil sample, an acrylic container (aquarium), a digital multimeter, aluminum plate electrodes, a DC power supply, and varying volumes of water up to 1200 mL.

Water was gradually added to the soil sample in increments, starting at 300 mL and increasing to 1200 mL. During each increment, the soil was subjected to three voltage variations: 10, 15 V, and 20 V. The resulting electric current was measured using a digital multimeter after each addition of water. The resistance (R) was then calculated using Ohm's Law, expressed as:

$$R = \frac{V}{I} \quad (2)$$

where:
R = Resistance (Ω)
V = Applied voltage (V)
I = Measured current (A)

3.5 Electrokinetic Remediation Setup

A total of 1500 g of dry soil was placed into a rectangular acrylic container measuring 30 cm × 10 cm × 10 cm. The soil was evenly compacted and divided into three equal segments (each 10 cm in length) to monitor the spatial distribution of Pb during remediation. Two aluminum plate electrodes (12 cm × 10 cm × 1 mm) were inserted at both ends of the container, with the anode placed at segment 3 and the cathode at segment 1. A direct current (DC) voltage of 20 V was continuously applied across the electrodes using a WANPTEK DC PSU 3010H power supply (maximum output current 5 A). The total treatment duration was set at two intervals: 24 hours and 48 hours.

Soil moisture was maintained at 900 mL throughout the treatment to ensure adequate electrical conductivity and simulate near-saturation field conditions, without causing water pooling. The electrical current was monitored every 4 hours using a Hioki DT4261 digital multimeter connected in series. No repetition was performed due to equipment limitations; therefore, this study serves as a preliminary investigation. The electrokinetic remediation system setup is illustrated in Figure 1.

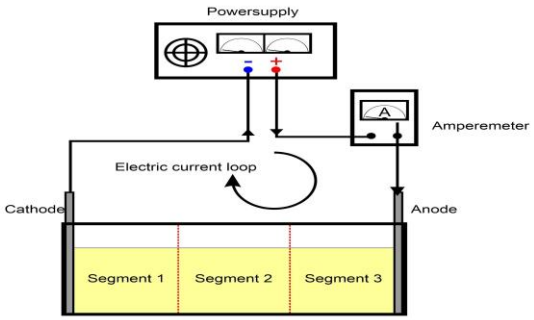


Figure 1 Electrokinetic circuit diagram

3.6 Pb Concentration Measurements

Pb concentration measurements were carried out before and after treatment. Soil samples were collected in each segment, up to 10 g. Soil sampling was conducted before and after treatment for 24 and 48 hours. Pb concentration was measured in soil to determine its distribution and movement during the research period. In addition, measurements of Pb concentration at each electrode were conducted to strengthen analysis of Pb sources in the soil and the potential for increasing Pb concentration due to Pb oxidation at the electrodes, driven by electrokinetic processes.

3.7 Soil pH Measurements

Soil pH was measured at 0, 24, and 48 hours using a pH meter. 10 g of soil was dissolved using 25 mL of distilled water. Next, let the soil settle, and the top layer of liquid will be clear. Dip the pH meter into the clear liquid from the soil sedimentation and record the soil pH value listed on the pH meter.

3.8 Analysis Data

Data analysis in this study used XRF measurements to determine Pb concentrations before and after treatment, along with soil pH measurements, resistance values, and WHC calculations. Data processing was carried out using Microsoft Excel, which was used to compile graphs of the relationship between water addition and resistance values, of Pb concentration in the soil in each segment, and of Pb concentration in the electrode.

3.9 Efficiency Calculation

The efficiency of Pb removal from soil during electrokinetic remediation was calculated to quantify ion migration and extraction in each soil segment, particularly the one adjacent to the cathode. The removal efficiency of Pb was calculated using a standard equation commonly applied in electrokinetic remediation studies (Reddy & Cameselle, 2009; Kim et al., 2014).

$$\text{Removal Efficiency (\%)} = \frac{C_0 - C_t}{C_0} \times 100\% \quad (3)$$

where:
C_0 = Initial concentration (ppm)
C_t = Final concentration (ppm)

III. RESULTS AND DISCUSSION

3.1 Water Holding Capacity (WHC) and Response of Water Addition to Circuit Current

Water-holding capacity (WHC) refers to a soil's ability to retain water, which is influenced by its mineral composition, texture, and structure (Rachman et al., 2019). WHC is a critical parameter in electrokinetic remediation, as soil must contain sufficient moisture to facilitate ionic conductivity. Without added moisture, the soil remains non-conductive even when an electric potential is applied.

Based on laboratory measurements, the WHC of the soil sample was determined to be 83.16%. This value corresponds to a maximum water retention of approximately 1247.4 mL for a 1500 g sample. The high WHC is attributed to the fine particle size of the soil, which passed through a 200 mesh. The fine texture increases surface area and pore connectivity, enabling greater water absorption and retention (Sefiana et al., 2022).

To identify the optimal moisture content, a series of preliminary tests was conducted in which water was incrementally added to the soil sample in 100 mL steps, ranging from 100 mL to 1200 mL. At each stage, the electrical current response was measured under a constant voltage. Based on these observations, 900 mL was selected as the operational water content, as the soil exhibited good absorption without surface pooling.

When water volume exceeded 900 mL (i.e., at 1000–1200 mL), the soil approached saturation, and free water began to accumulate on the surface. Under near-saturation or oversaturation conditions, the electroosmotic flow — which is the primary mechanism driving directed pore water movement in EKR — becomes less controlled, as excess surface water creates preferential flow pathways that bypass the soil matrix and disrupt the unidirectional transport of contaminant ions, potentially leading to undesirable redistribution of Pb^{2+} ions beyond the intended migration direction and reducing overall remediation efficiency (Acar & Alshawabkeh, 1993; Reddy & Cameselle, 2009).

3.2 Effect of adding water on resistivity values

The electrical resistance of the soil matrix is a key parameter for determining optimal operating conditions in electrokinetic remediation. Figure 2 illustrates the relationship between water volume and soil resistance across three applied voltage levels (10 V, 15 V, and 20 V). Across all voltage conditions, increasing the volume of added water from 300 mL to 1200 mL resulted in a clear, consistent decrease in resistance, indicating improved electrical conductivity.

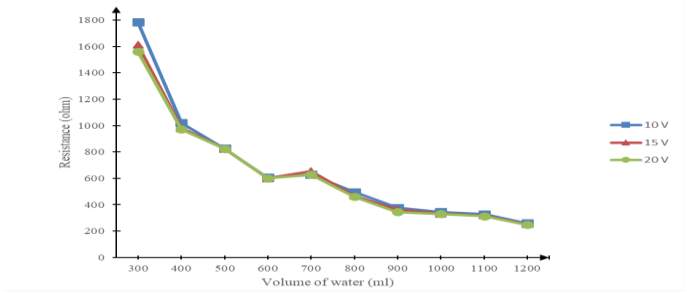


Figure 2 Resistance value

This trend is expected, as water serves as a medium for ionic conduction in soil. The presence of additional water increases pore water connectivity, reduces contact resistance between particles, and enhances the movement of charged species (Rohmannudin et al., 2018). As shown in Figure 2, the lowest resistance values were observed at 20 V, suggesting that higher voltage facilitated greater current flow at the same moisture content.

However, it should be noted that resistance is a property of the medium and does not depend directly on the applied voltage. Rather, the current (I) increases with voltage (V) when resistance (R) is

constant, according to Ohm's Law (Eq. 2.2). In this experiment, the decrease in resistance was driven by the increase in water content—not by voltage—although higher-voltage conditions revealed more pronounced current responses.

Between 900 mL and 1200 mL of water, the resistance curve began to plateau, indicating that the soil was near saturation and that further additions had minimal impact on conductivity. Beyond 900 mL, visible puddling was observed, potentially leading to non-uniform ion transport. Therefore, 900 mL was selected as the operational water volume to maintain good conductivity without causing oversaturation. The 20 V condition was selected as the main treatment due to its consistent association with the lowest resistance, thereby optimizing the electrokinetic potential for ion migration (Krcmar et al., 2017).

3.3 Soil pH Values

Changes in soil pH during electrokinetic remediation are closely related to electrochemical reactions at the electrodes. As shown in Table 1, soil pH varied across the three segments and the three treatment durations (0, 24, and 48 hours).

Table 1 Soil pH

Segment	pH		
	0 hours	24 hours	48 hours
1	7.82	8.09	9.23
2	7.86	8.05	7.95
3	7.82	8.00	7.69

Notes: pH 7,6-8,5 (slightly alkaline), pH > 8,5 (alkaline) (Soil and Fertilizer Instrument Standard Testing Center, 2023)

At the initial stage (0 hours), all segments showed slightly alkaline conditions, with pH values ranging from 7.82 to 7.86. After 24 hours of treatment, pH increased slightly in all segments, reaching 8.09 in segment 1, 8.05 in segment 2, and 8.00 in segment 3. However, after 48 hours, segment 1 exhibited a substantial increase to 9.23 (a 17.9% increase from the initial value), indicating strong alkalinity. In contrast, segments 2 and 3 showed a decrease in pH to 7.95 and 7.69, respectively, although both remained within the slightly alkaline range.

These pH shifts are caused by the electrolysis of water under an applied electric field. At the cathode (adjacent to segment 1), water reduction produces hydroxide ions (OH^-), which accumulate and raise the pH (Acar et al., 1990). At the anode (segment 3), water oxidation generates hydrogen ions (H^+), leading to acidification and a decline in pH. Segment 2, located midway between electrodes, experiences both OH^- and H^+ ion migration, resulting in intermediate pH values and fluctuations over time.

The pronounced alkalinity in segment 1 confirms the dominance of OH^- accumulation due to proximity to the cathode. Meanwhile, the pH value decline in segment 3 is attributed to H^+ enrichment, consistent with the expected electrochemical gradient. Segment 2 represents a transitional zone where ion interactions are more balanced, resulting in minor pH fluctuations. These findings align with the mechanisms reported by Acar et al. (1990) and highlight the spatial variability of electrokinetic effects within the soil matrix.

3.4 Pb Concentration in Soil and Electrodes

The Pb concentration in each soil segment at 0, 24, and 48 hours is shown in Figure 3. Initially (0 hours), Pb concentrations were relatively balanced across segments: segment 1 (165.0 ppm), segment 2 (158.9 ppm), and segment 3 (163.3 ppm). After 24 hours of electrokinetic remediation, Pb concentration slightly decreased in segments 1 and 3, while segment 2 showed a marginal increase: 159.5 ppm (seg. 1), 161.4 ppm (seg. 2), and 157.7 ppm (seg. 3). The decrease in segment 1 reflects the onset of electromigration, whereby positively charged Pb^{2+} ions are driven toward the negatively charged cathode under the applied electric field, followed by electrochemical reduction (Eq. 3.1) at the electrode surface. The temporary increase in segment 2 is attributed to transient ion accumulation in the

transitional zone, as Pb^{2+} ions migrating from segment 3 had not yet fully passed through toward the cathode, creating a momentary flux imbalance.

$$Pb^{2+} + 2e \rightarrow Pb \quad (4)$$

At 48 hours, a more distinct pattern emerged. Pb concentration continued to decline in segment 1 (155.1 ppm), remained stable in segment 2 (160.0 ppm), and increased in segment 3 (167.0 ppm). The continued reduction in segment 1 confirms the cumulative and time-dependent nature of electromigration and electroosmotic flow toward the cathode. Stabilization in segment 2 indicates a near-steady-state condition in which the rate of ion influx from segment 3 and efflux toward segment 1 approached equilibrium, consistent with dynamic buffer behavior described by Acar & Alshawabkeh (1993). The anomalous increase in segment 3 surpassing its initial concentration is attributed to anodic back-contamination, a phenomenon in which Pb originally present on the aluminum electrode surface undergoes oxidation (Eq. 3.2) and dissolves back into the surrounding soil. This process is further accelerated by the acidic microenvironment generated near the anode through water oxidation (Eq. 3.3), which enhances Pb solubility and promotes ion remobilization (Reddy & Cameselle, 2009).

$$Pb \rightarrow Pb^{2+} + 2e \quad (5)$$

$$2H_2O \rightarrow O_2 + 4H^+ + 4e^- \quad (6)$$

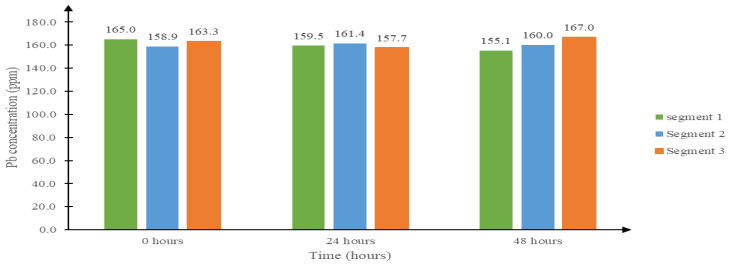


Figure 3 Pb Concentration in Soil

This distribution reflects the directional migration of Pb^{2+} ions under the influence of an applied electric field. Pb^{2+}, being positively charged, tends to move toward the cathode. The observed decrease in segment 1 — located closest to the cathode — confirms ion migration and partial removal from the soil. Based on the initial and final values, the total reduction in segment 1 was 9.9 ppm (or 6.0%). Meanwhile, the increase in segment 3 suggests possible remobilization of Pb^{2+} ions due to anodic dissolution of the electrode.

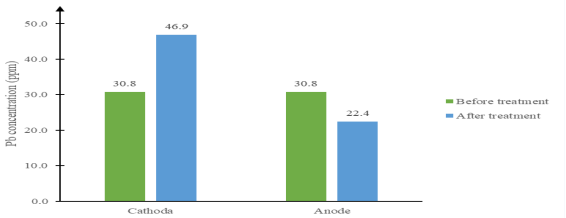


Figure 4 Pb Concentration on Electrode Plates (Cathode and Anode)

Figure 4 presents the Pb concentration on the cathode and anode surfaces. At the cathode, Pb concentration increased from 30.8 ppm to 46.9 ppm, indicating ion accumulation on the electrode via electromigration. In contrast, the Pb content on the anode dropped from 30.8 ppm to 22.4 ppm. This suggests that Pb originally present on the anode surface dissolved into the surrounding soil as soluble Pb^{2+} ions through the anodic oxidation reaction (Eq. 3.2).

This process is reinforced by the concurrent drop in pH in segment 3 and the visual changes on the anode surface (Figure 5), which exhibited a darker, patchy appearance typical of oxidized aluminum layers (Pourbaix et al., 1997; Riyanta & Rahmatullah, 2016). The acidic environment near the anode,

generated by H^+ ions from water oxidation, promotes further Pb dissolution. The presence of this secondary contamination pathway highlights a limitation in the use of reactive electrodes.

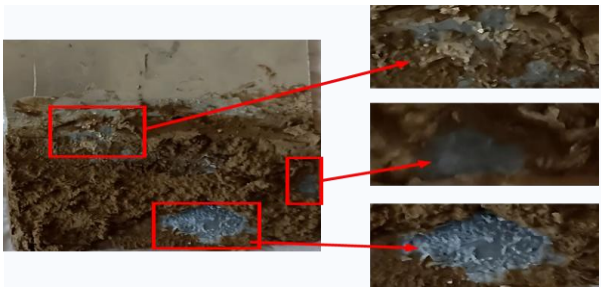


Figure 5 Photograph of the anode plate after 48 hours of electrokinetic remediation. (The image was taken using a smartphone camera — no magnification applied. Observable surface discoloration suggests oxidation of the aluminum electrode during treatment.)

These findings align with the theory proposed by Acar & Alshawabkeh (1993), wherein electrolysis near the electrodes creates pH gradients that influence metal solubility and migration. Segment 2, as the midpoint between electrodes, exhibited relatively stable Pb concentrations throughout, acting as a transitional buffer zone for migrating ions.

The removal efficiency at the cathode region (segment 1) was modest, with only 6% reduction over 48 hours. This relatively low value may be attributed to the short treatment duration, soil buffering capacity, and possible re-equilibration of metal ions. Nevertheless, the Pb increase at the cathode and the decrease in segment 1 clearly show that electromigration is active and functional.

To enhance removal efficiency, future applications may consider: Using inert electrodes (e.g., graphite or platinum-coated titanium) to minimize anode corrosion; Extending treatment time beyond 48 hours to allow more complete migration; Applying chelating agents such as EDTA or citric acid to improve Pb^{2+} mobility and reduce precipitation, as supported by Reddy & Cameselle (2009) and Kim et al. (2014).

In conclusion, electrokinetic remediation effectively initiates Pb^{2+} migration toward the cathode. However, releasing Pb from the anode via electrochemical oxidation remains a challenge, and optimization is needed to minimize secondary contamination and enhance long-term performance.

IV. CONCLUSION

This study demonstrated that electrokinetic remediation (EKR) effectively initiated Pb^{2+} migration in ex-mining soil from PT Semen Baturaja Tbk using aluminum plate electrodes at 20 V direct current. Soil pH shifts were spatially distinct: segment 1 (near cathode) became strongly alkaline (pH 9.23) due to OH^- accumulation, while segment 3 (near anode) became more acidic from H^+ generation, and segment 2 remained transitionally stable.

After 48 hours of treatment, Pb^{2+} concentration in segment 1 decreased by 9.9 ppm (6.0%), and cathode Pb accumulation increased from 30.8 to 46.9 ppm, confirming active electromigration. However, Pb concentration in segment 3 increased beyond its initial value due to anodic back-contamination caused by electrochemical oxidation of the aluminum electrode, compounded by the acidic anode environment. Although EKR demonstrated functional directional Pb^{2+} migration, the modest removal efficiency and secondary contamination from reactive electrodes highlight the need for further optimization, including the use of inert electrodes, extended treatment durations, and chelating agents, to support safer and more effective post-mining land reclamation.

ACKNOWLEDGEMENT

None.

CONFLICT OF INTEREST

The authors declare no conflict of interest.

FUNDING STATEMENT

This research received no specific funding.

DECLARATION OF GENERATIVE AI AND AI-ASSISTED TECNOLOGIES IN THE WRITING PROCESS

GPT was used solely to correct grammatical and typographical errors. The author bears full responsibility for the content and integrity of the publication.

REFERENCES

Acar, Y. B., Gale, R. J., Gregg, A., Hamed, J., & Wong, R. L. (1990). Electrochemical processing of soils: Theory of pH gradient development by diffusion. *Journal of Environmental Science and Health, Part A*, **25**(6), 687–714.

Acar, Y. B., & Alshawabkeh, A. N. (1993). Principles of electrokinetic remediation. *Environmental Science & Technology*, **27**(13), 2638–2647. https://doi.org/10.1021/es00049a002

Asuquo, F. E., & Bate, G. B. (2020). Bioaccumulation of heavy metals in mangoes (*Mangifera indica* L.) found in the vicinity of gold mining sites of Zamfara State, Nigeria. *Journal of Environmental Chemistry and Ecotoxicology*, **12**(1), 45–58. https://doi.org/10.5897/JECE2020.0464

Buta, M., Blaga, G., Paulette, L., Păcurar, I., Roșca, S., Borsai, O., Grecu, F., Sînziana, P. E., & Negrușier, C. (2019). Soil reclamation of abandoned mine lands by revegetation in Northwestern Part of Transylvania: A 40-year retrospective study. *Sustainability*, **11**(12), 3393. https://doi.org/10.3390/su11123393

Devi, R.C., Hemavathi, R., Ashwinkumar, S., Gowtham, B., Selvam, M., & Vijay Vignesh, A. (2023). Electrokinetic remediation for textile wastewater contaminated soil. *Global NEST Journal*, **25**(5), 83–89. https://doi.org/10.30955/gnj.004691

Hartati, A., Safaruddin, Bashir, M. Al, & Tirtaweningtias, S. (2023). Analysis of reclamation activities in PT. Semen Baturaja (Persero) Tbk. *UEEJ-Unbara Environmental Engineering Journal*, **3**(02). e-ISSN: 2723-5599.

Kim, W. S., Jeon, E. K., Jung, J. M., Jung, H. B., Ko, S. H., Seo, C. I., & Baek, K. (2014). Field application of electrokinetic remediation for multi-metal contaminated paddy soil using two-dimensional electrode configuration. *Environmental Science and Pollution Research*, **21**(6), 4482–4491. https://doi.org/10.1007/s11356-013-2424-0

Krcmar, D., Varga, N., Prica, M., Cveticanin, L., Zukovic, M., Dalmacija, B., & Corba, Z. (2018). Application of hexagonal two-dimensional electrokinetic system on the nickel-contaminated sediment and modelling the transport behavior of nickel during electrokinetic treatment. *Separation and Purification Technology*, **192**, 253–261. https://doi.org/10.1016/j.seppur.2017.10.008

Liu, L., Li, W., Song, W., & Guo, M. (2018). Remediation techniques for heavy metal-contaminated soils: Principles and applicability. *Science of the Total Environment*, **633**, 206–219. https://doi.org/10.1016/j.scitotenv.2018.03.161

Mungki, L. Y., & Taufikurahman. (2004). Effect of lead on mustard plant germination at concentrations according to the maximum lead content in Group B drinking water. *Ekologi & Biodiversitas Tropika*, **3**, 31–35.

Pourbaix, M., Zhang, H., & Pourbaix, A. (1997). Presentation of an atlas of chemical and electrochemical equilibria in the presence of a gaseous phase. *Materials Science Forum*, **251–254**, 143–148. https://doi.org/10.4028/www.scientific.net/MSF.251-254.143

Rachman, L. M., Baskoro, D. P. T., Wahjunie, E. D., Nurmilah, A., Astriani, T., & Dewi, N. M. (2019). Evaluation of physical soil properties controlling water-holding capacity and water supply to plants and their relation to agricultural management in suboptimal land. In S. Herlinda et al.

(Eds.), *Prosiding Seminar Nasional Lahan Suboptimal 2019, Palembang 4–5 September 2019* (pp. 111–120). Unsri Press.

Reddy, K. R., & Cameselle, C. (Eds.). (2009). *Electrochemical remediation technologies for polluted soils, sediments and groundwater*. John Wiley & Sons. https://doi.org/10.1002/9780470523650

Riyanta, B., & Rahmatullah, A. (2016). Corrosion analysis of orange peel-type aluminum roof with 0.8 mm thickness. *Semesta Teknika*, **8**(1), 30–46. https://doi.org/10.18196/st.v8i1.911

Rohmannudin, T. N., Sulistijono, & Arini, A. (2018). The effect of moisture content and soil type on current supply in an impressed current cathodic protection system for corrosion protection of steel pipes. *Jurnal Sains Materi Indonesia*, **18**(2), 49–54. https://doi.org/10.17146/jsmi.2017.18.2.4163

Sarie, H. (2019). Potential dangers of heavy metal contamination in the coal mine used land as agricultural land. *Buletin LOUPE*, **15**(02), 37-41. https://doi.org/10.51967/loupe.v15i02.213

Sefiana, R. R., Ma'shum, M., Padusung, & Tejowulan, S. (2022). Soil consistency index on various degraded lands in Kayangan District, North Lombok. *Journal of Soil Quality and Management*, **1**(2), 18–22. https://doi.org/10.29303/jsqm.v1i2.62

Siregar, H. A., Hasjim, M., & Juniah, R. (2020). Technical and economic evaluation of post-mining land reclamation at PT. Semen Indonesia (Persero) Tbk. *Jurnal Pertambangan*, **4**(1). https://ejournal.ft.unsri.ac.id/index.php/JP

SNI 03-1971-1990. (1990). Method of testing aggregate moisture content. National Standardization Agency of Indonesia.

Soil and Fertilizer Instrument Standard Testing Center. (2023). Technical manual for chemical analysis of soil, plants, water, and fertilizers (3rd ed.). Ministry of Agriculture, Indonesia.

Suied, A. A., Tajudin, S. A. A., Zakaria, M. N., & Madun, A. (2018). Potential electrokinetic remediation technologies of laboratory scale into field application: Methodology overview. *Journal of Physics: Conference Series*, **995**(1), 012083. https://doi.org/10.1088/1742-6596/995/1/012083

Yahaya, T., Umar, A., Abubakar, M., Abdulazeez, A., Musa, B., & Ibrahim, Y. (2023). Heavy metals in the soil around a cement company in Sokoto, Northwestern Nigeria, pose health risks. *Industrial and Domestic Waste Management,* **3**(1), 17–26. https://doi.org/10.53623/idwm.v3i1.183

Zulfiqar, W., Iqbal, M. A., & Butt, M. K. (2017). Pb^{2+} ions mobility perturbation by iron particles during electrokinetic remediation of contaminated soil. *Chemosphere*, **169**, 257–261. https://doi.org/10.1016/j.chemosphere.2016.11.083